

PHYSICAL METHODS
OF INVESTIGATION

Crystal Structure and Thermodynamic Properties
of Titanate $\text{ErGaTi}_2\text{O}_7$

L. T. Denisova^{a, *}, M. S. Molochev^{a, b}, V. V. Ryabov^c, Yu. F. Kargin^d,
L. G. Chumilina^a, and V. M. Denisov^a

^a Siberian Federal University, Krasnoyarsk, 660041 Russia

^b Kirenskii Institute of Physics, Federal Research Center “Krasnoyarsk Scientific Center”,
Siberian Branch, Russian Academy of Sciences, Krasnoyarsk, 660036 Russia

^c Institute of Metallurgy, Ural Branch, Russian Academy of Sciences, Yekaterinburg, 620016 Russia

^d Baikov Institute of Metallurgy and Material Science, Russian Academy of Sciences, Moscow, 119991 Russia

*e-mail: ldenisova@sfu-kras.ru

Received October 21, 2020; revised November 23, 2020; accepted November 30, 2020

Abstract—Erbium gallium titanate was prepared by solid-phase synthesis via the sequential calcination of precursor oxides in an air atmosphere at 1273 and 1573 K. The crystal structure of $\text{ErGaTi}_2\text{O}_7$ was characterized by full-profile analysis for the X-ray diffraction pattern of the synthesized powder sample as follows: space group *Pcnb*, $a = 9.77326(15)$ Å, $b = 13.5170(2)$ Å, $c = 7.33189(11)$ Å, $V = 918.58(3)$ Å³, $\rho = 6.10$ g/cm³. The high-temperature heat capacity of erbium gallium titanate was measured by differential scanning calorimetry within a temperature range of 320–1000 K. Based on these data, the basic thermodynamic functions of $\text{ErGaTi}_2\text{O}_7$ were calculated.

Keywords: erbium gallium titanate, solid-state synthesis, crystal structure, high-temperature heat capacity, thermodynamic functions

DOI: 10.1134/S0036023621040082

INTRODUCTION

Titanates of rare-earth elements $\text{R}_2\text{Ti}_2\text{O}_7$ ($\text{R} = \text{REE}$) attract the attention of researchers for a long time [1–7] due to the possibilities of their practical application. Nevertheless, many properties of the mentioned compounds are poorly studied, and this especially concerns complex titanates of rare-earth elements ($\text{R}'_x\text{R}''_x$) Ti_2O_7 , ($\text{R}', \text{R}'' = \text{REE}$) [8, 9] and RMTi_2O_7 ($\text{R} = \text{Sm}–\text{Lu}$, Y ; $\text{M} = \text{Ga}, \text{Fe}$) [10]. Thus, for example, the last paper communicates the synthesis of all the mentioned compounds, whereas the crystal structure was characterized only for one of them, i.e., $\text{GdGaTi}_2\text{O}_7$. The $\text{R}_2\text{O}_3–\text{Ga}_2\text{O}_3(\text{Fe}_2\text{O}_3)–\text{TiO}_2$ phase diagrams have not been completely constructed. To refine the phase ratios in such systems, it is necessary to have reliable data on the properties of formed oxides.

The present communication contains the data on the crystal structure and thermophysical properties (heat capacity and basic thermodynamic functions) of titanate $\text{ErGaTi}_2\text{O}_7$ within a temperature range of 320–1000 K.

EXPERIMENTAL

$\text{ErGaTi}_2\text{O}_7$ was synthesized from Er_2O_3 (chemically pure grade), Ga_2O_3 , and TiO_2 (specialty pure) by solid-state reactions. The synthesis method was described in the earlier paper [11]. The compositions of samples were monitored by X-ray diffraction analysis (Bruker D8 Advance diffractometer, Vantec linear detector, CuK_α radiation). X-ray diffraction experimental conditions are the same as described in [11].

The heat capacity of $\text{ErGaTi}_2\text{O}_7$ was measured by differential scanning calorimetry (STA 449 C Jupiter). Some specific features of these experiments were described in our papers [11–14].

RESULTS AND DISCUSSION

The X-ray diffraction pattern of synthesized polycrystalline $\text{ErGaTi}_2\text{O}_7$ at room temperature is shown in Fig. 1.

All reflections of the experimental X-ray diffraction pattern were indexed in an orthorhombic unit cell (space group *Pcnb*) with parameters close to the values for $\text{GdGaTi}_2\text{O}_7$ [10] (Rietveld refinement by the TOPAS 4.2 software [15]). When accomplishing this, the Gd ion was replaced by an Er ion. According to

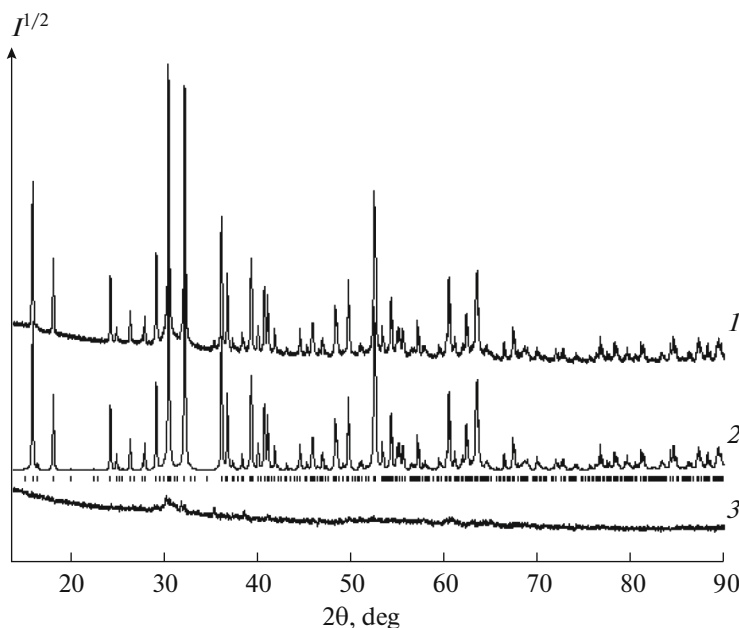


Fig. 1. X-ray diffraction pattern of $\text{ErGaTi}_2\text{O}_7$ at room temperature: (1) experimental, (2) calculated, and (3) difference profiles after Rietveld refinement with calculated locations of reflections (strokes).

[10], one Ga ion in the structure of $\text{GdGaTi}_2\text{O}_7$ is disordered over two positions: $4c$ (Ga) and $8d$ (Gai) with populations of 0.78 and 0.11, respectively. For this structure, we used powder refinement, which is less precise, so the mentioned populations were fixed. We have also taken into account the fact that three positions in the independent part of an initial $\text{GdGaTi}_2\text{O}_7$ model cell are populated by Ti/Ga. This disordering does not incorporate disordering over several positions as for the case of Ga/Gai. To improve stability in the refinement of the occupancies of Ti/Ga positions, a

constraint in the form of linear equation was imposed on the summary amount of Ti and Ga ions in a cell. The obtained results are listed in Tables 1–3. The linear dependence of the unit cell volume on the radius of rare-earth ions for RGaTi_2O_7 ($\text{R} = \text{Eu}, \text{Gd}, \text{Dy}, \text{Er}, \text{Lu}$) (Fig. 2) seems to confirm that the hypothetical chemical composition is close to the theoretical composition. The unit cell volumes of these compounds were determined by us, and the ionic radii of rare-earth ions were taken from [16].

The obtained experimental results on the high-temperature heat capacity of erbium gallium titanate (Fig. 3) show that C_p grows with an increase in temperature from 320 to 1000 K. The dependence $C_p = f(T)$ was described by the Maier–Kelley equation [17] as

$$C_p = a + bT - cT^{-2}. \quad (1)$$

In our case, it takes the following form (at a correlation coefficient of 0.9990 and a maximum deviation of experimental points from the fitting curve of 0.65%):

$$C_p = (255.85 \pm 0.43) + (30.9 \pm 0.5) \times 10^{-3}T - (39.11 \pm 0.42) \times 10^5 T^{-2}. \quad (2)$$

Due to the absence of other data on the heat capacity of $\text{ErGaTi}_2\text{O}_7$, comparison with $\text{Er}_2\text{Ti}_2\text{O}_7$ was carried out [18] (Fig. 3). The dependences $C_p = f(T)$ for erbium titanate and erbium gallium titanate are different. The heat capacity C_p of substituted titanate is lower at low temperatures and higher at high temperatures as compared to $\text{Er}_2\text{Ti}_2\text{O}_7$. It should be noted that

Table 1. Unit cell parameters of $\text{ErGaTi}_2\text{O}_7$ and $\text{GdGaTi}_2\text{O}_7$ *

Parameter	$\text{ErGaTi}_2\text{O}_7$ (our data)	$\text{GdGaTi}_2\text{O}_7$ [10]
Space group	<i>Pcnb</i>	<i>Pcnb</i>
a , Å	9.77321(15)	9.7804(3)
b , Å	13.5170(2)	13.605(1)
c , Å	7.33189(11)	7.4186(2)
V , Å ³	968.58(3)	987.16
ρ , g/cm ³	6.10	5.848
R_{wp} , %	3.97	
R_p , %	3.02	
R_B , %	0.81	
χ^2	1.62	

* a , b , c , β are the unit cell parameters, V is the unit cell volume, ρ is the calculated density, R_{wp} , R_p , and R_B are the weight profile, profile, and integral reliability factors, and χ^2 is the fitting quality.

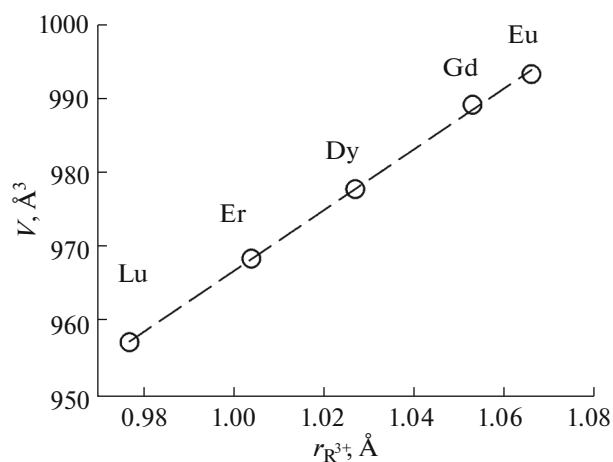


Fig. 2. Unit cell volume of $R\text{GaTi}_2\text{O}_7$ ($R = \text{Eu, Gd, Dy, Er, Lu}$) versus radius of rare-earth ions.

the partial substitution of erbium by gallium leads to the transformation of the crystal structure of titanate (space group $Fd\bar{3}m \rightarrow$ space group $Pcnb$). Hence, the substitution of a half of erbium atoms by gallium leads to the formation of $\text{ErGaTi}_2\text{O}_7$ with new individual physicochemical properties. This leads to both a difference between the absolute values of C_p and different $C_p = f(T)$ dependences.

The values found for $C_{p,298}$ by Eq. (2) can be compared with the values calculated by different model representations, namely, the additive Neumann–Kopp (NK) method [19, 20], the incremental Kumok method (IKM) [21], and the group contribution method (GCM) [22] (the calculation by Ivanova's

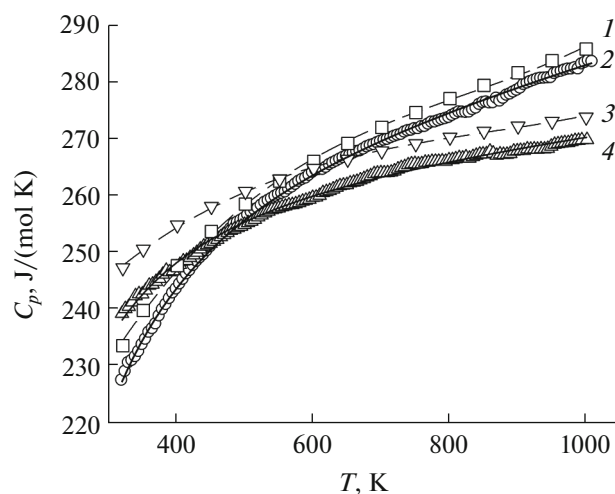


Fig. 3. Molar heat capacity: (2), (4) experimental data and (1), (3) values calculated by the group contribution method for (1), (2) $\text{ErGaTi}_2\text{O}_7$ and (3), (4) $\text{Er}_2\text{Ti}_2\text{O}_7$.

method [23] requires the $\text{ErGaTi}_2\text{O}_7$ melting temperature data which are unavailable in the literature) (Table 4). It was found that the Kumok method gave the best agreement with experiment. The required heat capacities of simple oxides (Er_2O_3 , Ga_2O_3 , and TiO_2) at 298 K for calculations by the NK method were taken from [19].

The group contribution method [22] makes it possible to predict the temperature dependence of the heat capacity of inorganic compounds. In this method, the coefficients of the temperature dependence

Table 2. Atomic coordinates and isotropic thermal parameters B_{iso} for the structure of $\text{ErGaTi}_2\text{O}_7$

Atom	x	y	z	$B_{\text{iso}}, \text{Å}^2$	O_{cc}
Er	0.2451(5)	0.13430(14)	0.0025(10)	0.43(12)	1
Ti1	0.2535(14)	0.3861(4)	0.499(3)	1.00(17)	0.856(16)
Ga1	0.2535(14)	0.3861(4)	0.499(3)	1.00(17)	0.144(16)
Ti2	0.5	0.25	0.251(2)	1.0(4)	0.727(56)
Ga2	0.5	0.25	0.251(2)	1.0(4)	0.273(56)
Ti3	0.0047(1)	0.4873(5)	0.2533(15)	1.0(3)	0.781(32)
Ga3	9.0047(10)	0.4873(5)	0.2533(15)	1.0(3)	0.219(32)
Ga	0	0.25	0.3348(15)	2.1(3)	0.78
Ga1	0.049(5)	0.290(4)	0.158(7)	2.1(3)	0.11
O1	0.1616(12)	0.3934(12)	0.236(4)	0.5(19)	1
O2	0.399(2)	0.1142(17)	0.257(4)	0.5(19)	1
O3	0.101(2)	0.1540(10)	0.238(5)	0.5(19)	1
O4	0.374(4)	0.282(3)	0.443(4)	0.5(19)	1
O5	0.367(3)	0.282(3)	0.055(4)	0.5(19)	1
O6	0.363(3)	0.494(3)	0.435(4)	0.5(19)	1
O7	0.381(3)	0.489(3)	0.063(4)	0.5(19)	1

Table 3. Selected bond lengths in the structure of $\text{ErGaTi}_2\text{O}_7^*$

Bond	$d, \text{Å}$	Bond	$d, \text{Å}$
Er–O2	2.41(3)	Ga–O3	1.78(2)
Er–O2 ⁱ	2.31(3)	Ga–O5 ^{iv}	2.12(3)
Er–O3	2.24(3)	Gai–O1	1.87(6)
Er–O3 ⁱ	2.47(3)	Gai–O3	2.00(6)
Er–O4 ⁱ	2.35(4)	Gai–O3 ^{vi}	1.75(6)
Er–O5	2.35(4)	Gai–O4 ⁱ	1.76(6)
Er–O6 ⁱⁱ	2.22(3)	(Ti2/Ga2)–O2	2.08(2)
Er–O7 ⁱⁱⁱ	2.42(3)	(Ti2/Ga2)–O4	1.92(4)
(Ti1/Ga1)–O1	2.13(4)	(Ti2/Ga2)–O5	1.99(3)
(Ti1/Ga1)–O1 ^{iv}	1.92(4)	(Ti3/Ga3)–O1	1.995(16)
(Ti1/Ga1)–O4	1.88(4)	(Ti3/Ga3)–O2 ^v	1.96(2)
(Ti1/Ga1)–O5 ^{iv}	1.88(4)	(Ti3/Ga3)–O3 ^{vi}	2.176(18)
(Ti1/Ga1)–O6	1.87(3)	(Ti3/Ga3)–O6 ^{vii}	1.97(3)
(Ti1/Ga1)–O7 ^{iv}	1.97(3)	(Ti3/Ga3)–O7 ^{vii}	1.84(3)

* Symmetry codes: (i) $-x + 1/2, y, z - 1/2$; (ii) $-x + 1/2, y - 1/2, -z + 1/2$; (iii) $x, y - 1/2, -z$; (iv) $-x + 1/2, y, z + 1/2$; (v) $-x + 1/2, y + 1/2, -z + 1/2$; (vi) $-x, -y + 1/2, z$; (vii) $x - 1/2, -y + 1, -z + 1/2$; (viii) $x - 1/2, -y + 1/2, z + 1/2$.

$$C_p = a + bT + cT^{-2} + dT^2 \quad (3)$$

for a certain compound are found by summing the ionic contributions of ions composing this compound (tabular values are given in [22]). Using this method, we calculated the temperature dependences of the heat capacity of $\text{ErGaTi}_2\text{O}_7$ and $\text{Er}_2\text{Ti}_2\text{O}_7$ (Fig. 3). The values calculated for $\text{ErGaTi}_2\text{O}_7$ almost coincide with experimental data throughout the entire range of studied temperatures. At the same time, the heat capacities C_p calculated for $\text{Er}_2\text{Ti}_2\text{O}_7$ are slightly higher than experimental results (Fig. 3), though the dependences $C_p = f(T)$ are symbate.

The group contribution method analysis proposed in [22] to predict the heat capacity of solid oxides was performed in [24]. The calculation of $C_{p,298}$ for 113 oxides has shown that the mean error is 4.3%, and the maximum error is 26.3%. It has been pointed out that this method can not distinguish structural polymorphs. Moreover, the calculation of the heat capacity of CaO , Al_2O_3 , and ThO_2 used as an example within a temperature range of 300–2400 K has demonstrated that C_p decreases at high temperatures. The latter is associated with a more negative value of the coefficient d from Eq. (3). Among the overall

number of analyzed cations (129), a negative contribution from the coefficient d is observed in 25 cases. Based on the performed analysis, the authors [24] have concluded that the group contribution method [22] does not always provides reliable prediction for the $C_p = f(T)$ dependence. This method can yet be used to calculate temperature-dependent heat capacities in a small range of temperatures (below 1000 K) for solid compounds: for complex oxides when some additional information is unavailable. For such prediction, other methods require that, e.g., the melting temperature and $C_{p,298}$ (in the Kubaschewsky method) [25–28], one experimental heat capacity value and a temperature series of heat capacity of a reference (in the Erdos–Cherny method [25]), etc. be known. Moreover, using this method and the tables [29], it is possible to calculate $\Delta_f H_{298}^\circ$ and $\Delta_f G_{298}^\circ$. They are equal to -3274.2 ± 93.9 and -3089.4 ± 112.0 kJ/mol, respectively. The errors of calculations were determined by the error additivity rule.

Using the experimental data on $C_p = f(T)$ for $\text{ErGaTi}_2\text{O}_7$, its basic thermodynamic functions were calculated (Table 5).

CONCLUSIONS

The crystal structure of $\text{ErGaTi}_2\text{O}_7$ was refined by the full-profile analysis of the X-ray diffraction pattern of this complex oxide as follows: space group $Pcnb$; $a = 9.77326(15)$ Å, $b = 13.5170(2)$ Å, $c = 7.33189(11)$ Å; the atomic coordinates, the occupancies of positions, and the isotropic thermal parameters

Table 4. Comparison of the experimental heat capacities calculated at 298 K with the values calculated by model representations for $\text{ErGaTi}_2\text{O}_7$ (J/(mol K))

$C_p, (2)$	NK	$\Delta, \%$	IKM	$\Delta, \%$	GCM	$\Delta, \%$
221.0	211.4	–4.3	218.6	1.1	228.0	+3.2

Table 5. Thermodynamic properties of ErGaTi₂O₇

T, K	C_p , J/(mol K)	$H^\circ(T) - H^\circ(320 \text{ K})$, kJ/mol	$S^\circ(T) - S^\circ(320 \text{ K})$, J/(mol K)	$-\Delta G/T^*$, J/(mol K)
320	227.5	—	—	—
350	234.7	6.938	20.72	0.897
400	243.8	18.91	52.69	5.404
450	250.4	31.28	81.80	12.30
500	255.7	43.93	108.5	20.60
550	259.9	56.83	133.0	29.72
600	263.5	69.92	155.8	39.29
650	266.7	83.17	177.0	49.08
700	269.5	96.58	196.9	58.94
750	272.1	110.1	215.6	68.76
800	274.5	123.8	233.2	78.50
850	276.7	137.6	249.9	88.10
900	278.8	151.4	265.8	97.53
950	280.9	165.4	280.9	106.8
1000	282.8	179.5	295.4	115.9

* $\Delta G/T = [H^\circ(T) - H^\circ(320 \text{ K})]/T - [S^\circ(T) - S^\circ(320 \text{ K})]$.

of atoms in a unit cell were determined. Its heat capacity was measured at high temperatures (320–1000 K), and thermodynamic properties were determined.

ACKNOWLEDGMENTS

The authors are grateful to the Krasnoyarsk Regional Shared Facilities Center “Krasnoyarsk Scientific Center” (Siberian Branch, Russian Academy of Sciences).

CONFLICT OF INTERESTS

The authors declare that they have no conflict of interests.

REFERENCES

1. K. I. Portnoi and N. I. Timofeeva, *Oxygen Compounds of Rare Earth Elements* (Metallurgiya, Moscow, 1986) [in Russian].
2. A. G. Shcherbakova, L. G. Mamsurova, and G. E. Sukhanova, *Usp. Khim.* **48**, 423 (1979) 423.
3. L. N. Komissarova, V. M. Shatskii, G. Ya. Pushkina, et al., *Compounds of Rare-Earth Elements. Carbonates, Oxalates, Nitrates, and Titanates* (Nauka, Moscow, 1984) [in Russian].
4. W. Zhang, L. Zhang, H. Zhong, et al., *Mater. Characteriz.* **61**, 154 (2010).
<https://doi.org/10.1016/j.matchar.2009.11.005>
5. J. M. Farmer, L. A. Boatner, B. C. Chakoumakos, et al., *J. Alloys Compd.* **605**, 63 (2014).
6. C. G. Liu, L. J. Chen, D. Y. Yang, et al., *Comput. Mater. Sci.* **114**, 233 (2016).
7. J. Shamblin, C. L. Tracy, R. C. Ewing, et al., *Acta Mater.* **117**, 207 (2016).
<https://doi.org/10.1016/j.actamat.2016.07.017>
8. C. Chen, Z. Gao, H. Yan, et al., *J. Am. Ceram. Soc.* **99**, 523 (2016).
<https://doi.org/10.1111/jacs.13970>
9. Z. Gao, B. Shi, H. Ye, et al., *Adv. Appl. Ceram.* **144**, 191 (2014).
10. E. A. Genkina, V. I. Andrianov, E. L. Belokoneva, et al., *Kristallografiya* **36**, 1408 (1991). 1408.
11. L. T. Denisova, M. S. Molokeev, L. G. Chumilina, et al., *Inorg. Mater.* **56**, 1242 (2020).
12. L. T. Denisova, L. A. Irtyugo, Yu. F. Kargin, et al., *Inorg. Mater.* **53**, 93 (2017).
13. L. T. Denisova, L. A. Irtyugo, N. V. Belousova, et al., *Russ. J. Phys. Chem.* **93**, 598 (2019).
14. L. T. Denisova, L. A. Irtyugo, Yu. F. Kargin, et al., *Russ. J. Inorg. Chem.* **64**, 1161 (2019).
15. Bruker AXS TOPAS 4V: General Profile and Structure Analysis Software for Powder Diffraction Data. User's Manual (Bruker, Karlsruhe, 2008).
16. R. D. Shannon, *Acta Crystallogr., Sect. A* **32**, 751 (1976).
17. C. G. Maier and K. K. Kelley, *J. Am. Chem. Soc.* **54**, 3243 (1932).
18. L. T. Denisova, A. D. Izotov, Yu. F. Kargin, et al., *Dokl. Phys. Chem.* **475**, 139 (2017).
19. J. Leitner, P. Chuchvalec, D. Sedmidubsky, et al., *Thermochim. Acta* **395**, 27 (2002).

20. J. Leitner, P. Vonka, D. Sedmidubsky, et al., *Thermochim. Acta* **497**, 7 (2010).
21. V. N. Kumok, *Direct and Inverse Problems of Chemical Thermodynamics* (Nauka, Novosibirsk, 1987) [in Russian].
22. A. T. M. G. Mostafa, J. M. Eakman, M. M. Montoya, et al., *Ind. Eng. Chem. Res.* **35**, 343 (1996).
23. L. I. Ivanova, *Zh. Neorg. Khim.* **35**, 1809 (1961).
24. J. Leitner, D. Sedmidubsky, and P. Chuchvalec, *Ceram.-Silikaty* **46**, 29 (2002).
25. A. G. Morachevskii, I. B. Sladkov, and E. G. Firsova, *Thermodynamic Calculations in Chemistry and Metallurgy* (Lan', St. Petersburg, 2018) [in Russian].
26. P. J. Spencer, *Thermochim. Acta* **314**, 1 (1998).
27. G. K. Moiseev, N. A. Vatolin, L. A. Marshuk, et al., *Temperature-Dependent Reduced Gibbs Energies of Some Inorganic Substances (Alternative Data Bank AS-TRA.OWN)* (UrO RAN, Ekaterinburg, 1987) [in Russian].
28. O. Kubaschewski and C. B. Alcock, *Metallurgical Thermochemistry* (Pergamon, 1979; Metallurgiya, Moscow, 1982).
29. A. T. M. G. Mostafa, J. M. Eakman, and S. L. Yarbrow, *Ind. Eng. Chem. Res.* **34**, 4577 (1995).

Translated by E. Glushachenkova